Cation Distribution in Mixed Alkali Disilicate Glasses

P. Florian,[†] K. E. Vermillion,[†] P. J. Grandinetti,*[,†] I. Farnan,[‡] and J. F. Stebbins[§]

Contribution from the Department of Chemistry, The Ohio State University, 120 West 18th Avenue, Columbus, Ohio 43210-1173, Centre de Recherches sur la Physique des Hautes Températures, 1D Av. de la Recherche Scientifique, 45071 Orléans CEDEX 2, France, and Department of Geological and Environmental Sciences, Stanford University, Stanford, California 94305

Received November 22, 1995[⊗]

Abstract: We have investigated the structure of five disilicate glass compositions—$K_2O{\cdot}2SiO_2$, $(Na_{0.25}K_{0.75})_2O{\cdot}2SiO_2$, $(Na_{0.50}K_{0.50})_2O{\cdot}2SiO_2$, $(Na_{0.75}K_{0.25})_2O{\cdot}2SiO_2$, and $Na_2O{\cdot}2SiO_2$—using 2D ^{17}O Dynamic Angle Spinning (DAS) Nuclear Magnetic Resonance (NMR). The nonbridging and bridging oxygen sites can be resolved in the isotropic ^{17}O DAS spectrum. The bridging oxygen isotropic resonance shifts from 16.1 ppm in $K_2O{\cdot}2SiO_2$ to 11.8 ppm in $Na_2O{\cdot}2SiO_2$ and remains almost identical in width. The nonbridging oxygen isotropic line shapes in the mixed compositions are broader with a maximum intensity that continuously shifts from the position found in the pure potassium composition to the position found in the pure sodium composition. The evolution of the nonbridging oxygen isotropic line shape with changing alkali composition is consistent with a model of the glass structure where four alkali cations are distributed in random combinations around each nonbridging oxygen.

Introduction

The recent advent of solid-state NMR techniques, like Dynamic-Angle Spinning (DAS)[1−7] which provide high resolution solid-state NMR spectra of quadrupolar nuclei, is giving new insight into the structure of glasses.[8−11] One of the areas where this technique can provide a fresh view of an old problem is the mixed alkali effect. In the "mixed alkali effect" a linear addition in alkali ions of a second type into a single alkali silicate glass changes by an order of magnitude the electrical conductivity and the viscosity of the glass in a nonlinear fashion.[12] At present, there is considerable debate over the mechanism for this effect. Current theories of the "mixed alkali effect" in glasses rely heavily upon various models of the glass structure.[13,14] The Modified Random Network model[15,16] postulates the existence of nanoscaled zones composed of pure v-SiO_2 surrounded by alkali channels. The Cluster Bypass model[17] describes the glass structure as a network of microdomains (with a size of ≈5 nm) connected by a "tissue" of a different compositions. The Mixed-Alkali Defect model[18] relies on the existence of dedicated cation sites into which foreign cations can be locked. Since few experiments are available for investigating topological order and disorder in glasses, no particular model has yet been completely confirmed from experimental techniques.

The ternary system $Na_2O-K_2O-SiO_2$ is known to exhibit all the characteristics of the "mixed alkali effect"[12] and has been studied by scattering[19,20] and computational techniques.[21,22] In this paper we investigate this model system using ^{17}O DAS NMR. This nucleus can monitor the short range structure modifications in those alkali disilicate glasses as the composition changes from one single alkali to another. The nonbridging oxygen sees most if not all of the two types of network modifying cations and thus provides valuable information about their distribution in the glass. Related changes in the SiO_4 network can be directly monitored through the position and width of the bridging oxygen resonances.

Experimental Section

Sample Preparation and Characterization. The five glass compositions synthesized were $K_2O{\cdot}2SiO_2$, $(Na_{0.25}K_{0.75})_2O{\cdot}2SiO_2$,

* Author to whom correspondence should be addressed.
† The Ohio State University.
‡ Centre de Recherches sur la Physique des Hautes Températures.
§ Stanford University.
⊗ Abstract published in *Advance ACS Abstracts,* March 15, 1996.

(1) Samoson, A.; Lippmaa, E.; Pines, A. *Mol. Phys.* **1988**, *65*, 1013.
(2) Llor A.; Virlet, J. *Chem. Phys. Lett.* **1988**, *152*, 248.
(3) Chmelka, B. F.; Mueller, K. T.; Pines, A.; Stebbins, J.; Wu, Y.; Zwanziger, J. W. *Nature* **1989**, *339*, 42.
(4) Mueller, K. T.; Sun, B. Q.; Chingas, G. C.; Zwanziger, J. W.; Terao, T.; Pines, A. *J. Magn. Reson.* **1990**, *86*, 470.
(5) Grandinetti, P. J.; Baltisberger, J. H.; Llor, A.; Lee, Y. K.; Werner, U.; Eastman, M. A.;Pines, A. *J. Magn. Reson. A* **1993**, *103*, 72.
(6) Grandinetti, P. J.; Lee, Y. K.; Baltisberger, J. H.; Sun, B. Q.; Pines, A. *J. Magn. Reson. A* **1993**, *102*, 195.
(7) Grandinetti, P. J. Dynamic-angle spinning and applications. In *Encyclopedia of Nuclear Magnetic Resonance*; Grant, David M., Harris, Robin K., Eds.; John Wiley & Sons, 1995; and references cited therein.
(8) Farnan, I.; Grandinetti, P. J.; Baltisberger, J. H.; Stebbins, J. F.; Werner, U.; Eastman, M. A.; Pines, A. *Nature* **1992**, 358, 31−35.
(9) Youngman, R. E.; Zwanziger, J. W. *J. Non-Cryst. Solids* **1994**, *168*, 293−297.
(10) Youngman, R. E.; Zwanziger, J. W. *J. Am. Chem. Soc.* **1995**, *117*, 1397.
(11) Tagg, S. L.; Youngman, R. E.; Zwanziger, J. W. *J. Phys. Chem.* **1995**, *99*, 5111.
(12) Isard, J. O. *J. Non-Cryst. Solids* **1969**, *1*, 235--261.
(13) Day, D. E. *J. Non-Cryst. Solids* **1976**, *21*, 343−372.
(14) LaCourse, W. C.; Cormack, A. *Transaction ACA* **1991**, *27*, 211−224.
(15) Greaves, G. N. *J. Non-Cryst. Solids* **1985**, *71*, 171.
(16) Greaves, G. N. Glass structure and ionic transport. In *The Physics of Non-Crystalline Solids*; Pye, L. D., LaCourse, W. C., Stevens, H. J., Eds.; Taylor and Francis: London, 1992; pp 453−459.
(17) Ingram, M. D. *Philos. Mag. B* **1989**, *60*(6), 729−740.
(18) LaCourse, W. C. *J. Non-Cryst. Solids* **1987**, *95* & *96*, 905−912.
(19) Greaves, G. N.; Fontaine, A.; Lagarde, P.; Raoux, D.; Gurman, S. J. *Nature* **1981**, *293*, 611−615.
(20) Imaoka, M.; Hasegawa, H.; Yasui, I. *Phys. Chem. Glasses* **1983**, *24*(3), 72−78.
(21) Huang, C.; Cormack, A. N. *J. Chem. Phys.* **1990**, *93*(11), 8180−8186.
(22) Huang, C.; Cormack, A. N. *J. Chem. Phys.* **1991**, *95*(5), 3634−3642.

0002-7863/96/1518-3493$12.00/0

$(Na_{0.50}K_{0.50})_2O{\cdot}2SiO_2$, $(Na_{0.75}K_{0.25})_2O{\cdot}2SiO_2$, and $Na_2O{\cdot}2SiO_2$. These will be further denoted as v-Na_0K_{100}, v-$Na_{25}K_{75}$, v-$Na_{50}K_{50}$, v-$Na_{75}K_{25}$, and v-$Na_{100}K_0$, respectively. v-$Na_{100}K_0$ and v-Na_0K_{100} were synthesized from alkali carbonates and ^{17}O-enriched amorphous SiO_2. The SiO_2 was synthesized by hydrolysis of $SiCl_4$ with 40% ^{17}O-labeled H_2O, followed by drying at 1000 °C in an argon atmosphere. Reagents were carefully mixed by grinding, with 0.1 wt% CoO added to enhance spin−lattice relaxation. Mixtures were decarbonated overnight at about 700 °C, then melted for 1 h at 1100 to 1200 °C. Glasses were quenched by dipping the platinum crucible bottoms in water. Weight losses were carefully monitored and indicate that final compositions are within about 1% of nominal. The v-$Na_{25}K_{75}$, v-$Na_{50}K_{50}$, and v-$Na_{75}K_{25}$ glasses were made by melting together appropriate amounts of the two end member compositions.

NMR Spectroscopy. All experiments were performed on a Chemagnetics 9.4 T NMR spectrometer using a modified version of a homebuilt DAS probe described earlier.[23] All experiments were done at ambient temperature with sample spinning rates between 11 and 12 kHz. ^{17}O T_1 relaxation times were estimated using saturation recovery experiments under MAS conditions and assuming a single exponential recovery as first approximation. No differences in T_1 were observed between the bridging and nonbridging oxygen sites and the recycle delays were then adjusted to get at least 80% of signal recovery. The DAS angle pair (37.38°, 79.19°) was employed in removing the second-order anisotropic broadenings. The DAS pulse sequence employed was a hypercomplex shifted echo DAS sequence.[24] A DAS rotor reorientation time of 40 ms was used. To ensure selectivity of the ^{17}O central transition, suitable adjustment of the RF output power has been made so that the $\pi/2$ time measured on the solid sample and on the reference solution satisfied the relationship $(\pi/2)_{sld} \approx {}^1/_3(\pi/2)_{sol}$. The DAS echo[24] was shifted by an integer number of rotor periods. The two-dimensional ^{17}O DAS spectra for all five compositions are shown in Figure 1, and the five isotropic one-dimensional projections are shown in Figure 2. Table 1 summarizes the various experimental parameters used for the DAS experiments for the five compositions under investigation. The t_1 dimension was zero-filled to 256 points and no apodization was applied to this dimension to retain the highest resolution possible.

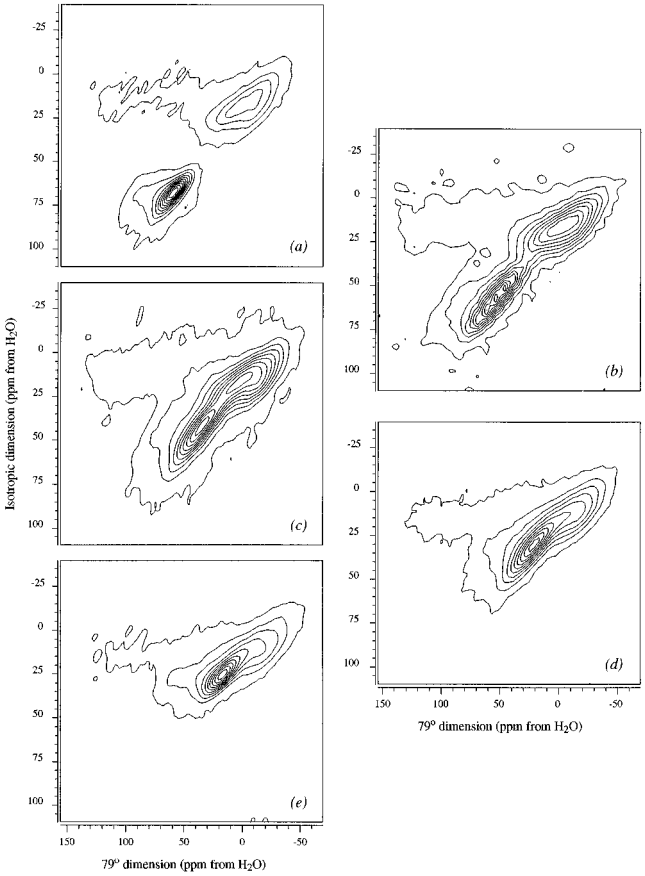

Figure 1. Two-dimensional 9.4 T ^{17}O DAS spectra of (a) v-$K_{100}Na_0$, (b) v-$K_{75}Na_{25}$, (c) v-$K_{50}Na_{50}$, (d) v-$K_{25}Na_{75}$, and (e) v-K_0Na_{100}. In each spectrum 10 equally spaced contour lines are drawn at levels ranging from 3 to 93% of the maximum intensity in the spectrum.

Discussion

The resonances for the bridging and nonbridging oxygens are clearly resolved in the two-dimensional spectrum of v-$K_{100}Na_0$ shown in Figure 1. As expected, the width in the anisotropic dimension, which is dominated by second-order quadrupolar broadenings, is smaller for the nonbridging oxygen since its bonding is more ionic than the bridging oxygen.[8,25] This assignment is further confirmed by the evolution of each peak while changing the composition: the bridging oxygen peak remains almost unchanged in position and the nonbridging oxygen peak moves to lower frequency (higher shielding) by addition of sodium in the glass. This behavior is expected since the ^{17}O chemical shifts in alkaline-earth metasilicates[25] and in the group II oxides[26] have been shown to increase with the cation ionic radius (Ahrens ionic radii:[27] 0.97 Å for Na and 1.33 Å for K), with a more marked dependence for the nonbridging oxygen than for the bridging oxygen.

The observed isotropic position δ_{obs} is defined by:

$$\delta_{obs} = \delta_{iso}^{CS} + \delta_{iso}^{2Q} \quad (1)$$

where δ_{iso}^{CS} is the isotropic chemical shift and δ_{iso}^{2Q} is the second-order quadrupolar isotropic shift, both expressed in ppm. For a spin I with a Larmor frequency ν_L, a nuclear quadrupole coupling constant C_Q and a quadrupolar asymmetry parameter η, δ_{iso}^{2Q} is defined by:

$$\delta_{iso}^{2Q}\,(\text{ppm}) = -\frac{3}{40}\left(\frac{C_Q}{\nu_L}\right)^2 \frac{I(I+1) - 3/4}{I^2(2I-1)^2}\left(1 + \frac{\eta^2}{3}\right) \times 10^6 \quad (2)$$

The observed position is therefore a function of both the isotropic chemical shift and the quadrupolar parameters.

There is very little variation of the bridging oxygen isotropic line shape with changes in composition. In addition, the mean isotropic shift varies from 16.1 to 11.8 ppm in going from the potassium to the sodium composition. This may be an effect of the alkali cations, and/or changes in the Si−O−Si bond angle distribution, and/or ring size distribution. Significant variations in the bridging oxygen anisotropic lineshape across the isotropic line shape can be seen for each composition. As previously shown,[8,28] these variations are attributed to a continuous distribution in C_Q and η for the bridging oxygens. These distributions can be correlated to changes in Si−O−Si bond angle,[8,28] and in principle, can be used to map the isotropic line shape of the bridging oxygen into the Si−O−Si bond angle distribution for these glasses. Unfortunately, the detection angle (79.19°) used in these experiments hinders this analysis due to the probable presence of chemical shift anisotropy that complicates the line shape fitting procedure. Ignoring the chemical shift anisotropy and fitting for quadrupolar anisotropy alone

(23) Eastman, M. A.; Grandinetti, P. J.; Lee, Y. K.; Pines, A. *J. Magn. Reson.* **1992**, 98, 333.
(24) Grandinetti, P. J.; Baltisberger, J. H.; Llor, A.; Lee, Y. K.; Werner, U.; Eastman, M. A.; Pines, A. *J. Magn. Reson. A* **1993**, *103*, 72.
(25) Timken, H. K. C.; Schramm, S. E.; Kirkpatrick, R. J.; Oldfield, E. *J. Phys. Chem.* **1987**, *91*, 1054−1058.
(26) Turner, G. L.; Chung, S. E.; Oldfield, E. *J. Magn. Reson.* **1985**, *64*, 316−324.
(27) Shannon, R. D.; Prewitt, C. T. *Acta Crystallogr.* **1969**, *B25*, 925−946.
(28) Grandinetti, P. J., Baltisberger, J. H.; Farnan, I.; Stebbins, J. F.; Werner, U.; Pines, A. *J. Phys. Chem.* **1995**, *99*, 12341.

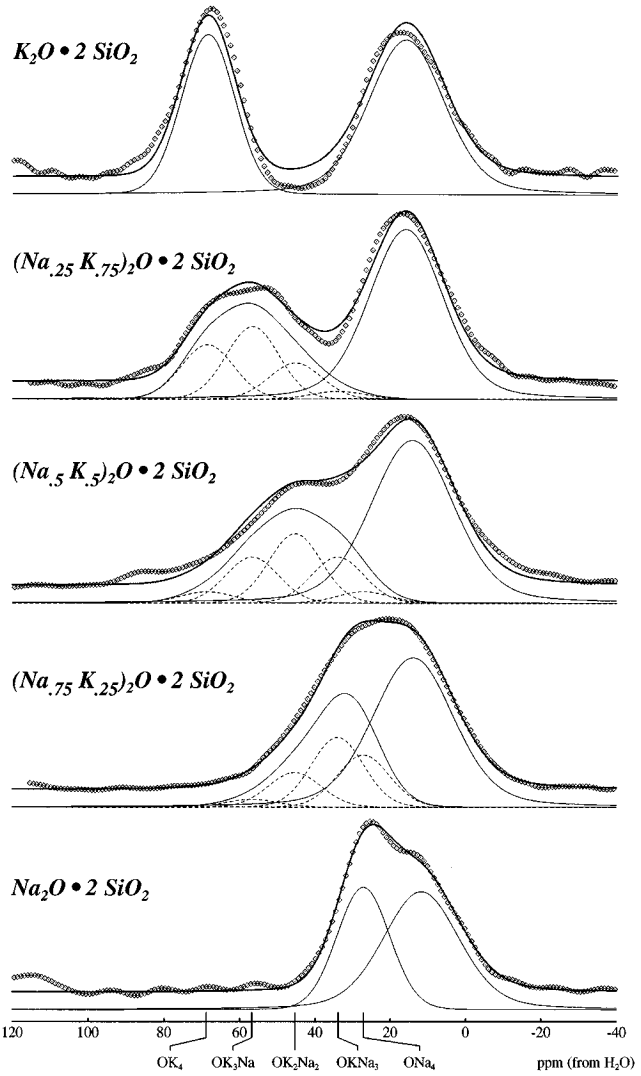

Figure 2. From top to bottom are the one-dimensional isotropic 9.4 T ^{17}O DAS spectra of v-$K_{100}Na_0$, v-$K_{75}Na_{25}$, v-$K_{50}Na_{50}$, v-$K_{25}Na_{75}$, and v-K_0Na_{100}. The experimental data are shown as diamonds, the simulation as a straight line, and each component as dashed lines, assuming a binomial distribution (see text).

Table 1. Experimental Conditions Used for the DAS Experiments

composition	T_1 (s)	rec delay (s)	T_{90} at 37 °C (μs)	T_{90} at 79 °C (μs)	t_1 dwell times (μs)	no. of scans	$t_1 \times t_2$
v-Na_0K_{100}	0.3	0.4	22.5	14.0	40	4096	46 × 256
v-$Na_{25}K_{75}$	3.0	5.0	15.0	15.0	40	1024	30 × 256
v-$Na_{50}K_{50}$	1.8	3.0	22.5	14.0	40	4096	38 × 256
v-$Na_{75}K_{25}$	2.5	3.0	15.0	15.0	40	2048	32 × 256
v-$Na_{100}K_0$	0.4	0.5	22.5	14.0	40	4096	71 × 256

would lead to inflated quadrupolar coupling constants and be interpreted as larger Si−O−Si angles. To eliminate the interference from chemical shift anisotropy and obtain accurate quadrupolar coupling parameters for the bridging oxygens magic-angle-spinning detected DAS[28,29] would be required.

For all compositions the anisotropic line shapes of the nonbridging oxygen sites are constant as a function of isotropic frequency. Assuming that the anisotropic line shape of the nonbridging oxygen resonance is dominated by second-order quadrupolar broadenings, this implies that there is little variation in the nuclear quadrupolar coupling constant C_Q and quadrupolar asymmetry parameter η for the nonbridging oxygen sites. We can therefore conclude that the observed broadening in the isotropic dimension for the nonbridging oxygen is dominated by isotropic chemical shift dispersion.

Table 2. Results of the Fit of the Isotropic Projection of the 2D ^{17}O DAS Spectra of (a) v-$K_{100}Na_0$, (b) v-$K_{75}Na_{25}$, (c) v-$K_{50}Na_{50}$, (d) v-$K_{25}Na_{75}$, and (e) v-K_0Na_{100}

composition	δ_{BO} (ppm)	$\Delta\nu_{BO}$ (Hz)	G/L_{BO}	δ_{NBO} (ppm)	$\Delta\nu_{NBO}$ (Hz)	G/L_{NBO}	BO/NBO (%)
v-$K_{100}Na_0$	16.1	1276	1.0	68.7	937	1.0	55/45
v-$K_{75}Na_{25}$	16.3	1336	0.8	58.9	1563	1.0	62/38
v-$K_{50}Na_{50}$	15.6	1579	0.7	46.4	1592	0.3	62/38
v-$K_{25}Na_{75}$	12.5	1414	0.9	31.0	1676	0.8	59/41
v-K_0Na_{100}	11.8	1207	0.6	27.0	839	0.6	56/44

[a] δ is the position of the maximum, $\Delta\nu$ is the full width at half maximum, $x = G/L$ refers to the x × Gaussian + $(1 - x)$ × Lorentzian shape, and BO/NBO is the calculated ratio of bridging over nonbridging.

The influence of the alkali cation on the nonbridging oxygen peak position is clearly seen in the five isotropic projections shown in Figure 2. Although there is a progressive overlap of the bridging and nonbridging oxygen peaks as the sodium content increases, it is still possible to deconvolute each of the five spectra into two components. Table 2 summarizes the "best" fits results assuming a mixture of Gaussian and Lorentzian line shapes. In all cases, the ratio of the integrated areas for the bridging and nonbridging oxygens falls reasonably close the 60/40 expected ratio for a disilicate composition.

Typical nonbridging oxygen isotropic line widths in the crystalline state are on the order of 200 Hz. For both the pure sodium and potassium compositions, the line width is ≃900 Hz, indicating that the disorder around the nonbridging oxygen is of the same extent for both compositions. This width results from the disorder around the nonbridging oxygen sites which produces a distribution in isotropic chemical shifts. Since there is a unique type of alkali cation present in those two glasses, the observed broadening reflects a disorder in the length and orientation of the alkali cation−nonbridging oxygen internuclear vector. This can be related to the spread of cation-oxygen distances R_{M-O} (and therefore oxygen−cation distance R_{O-M}) of ≈±0.5 Å observed by EXAFS in sodium, potassium, and cesium disilicate glasses.[19,30]

The nonbridging oxygen line shapes in the mixed compositions are almost twice as large as those in the pure glasses. To understand this behavior we assume that the nonbridging oxygen is 5-fold coordinated in the five glasses under study, i.e., the nonbridging oxygen is coordinated by 1 silicon and 4 alkalis. This assumption is supported by EXAFS studies of several alkali silicates[30] that led to the idea that the nonbridging oxygen coordination number lies between 4 and 6, closely matching the alkali coordination number. Related studies[19] as well as Molecular Dynamic calculations[31] have also shown that the coordination number of sodium in v-K_0 Na_{100} is 5 ± 0.5. In addition, a later study suggested that the cation coordination number is not changed by addition of potassium, and that strong similarities in the structure of the cation and the nonbridging oxygen clusters has been found[22] between sodium and potassium disilicate glasses. Therefore, with this fixed coordination number, only a limited number of nonbridging oxygen types can be created in the mixed composition: Si−O−Na_4, Si−O−Na_3K, Si−O−Na_2K_2, Si−O−NaK_3, and Si−O−K_4.

Since we know that δ_{iso}^{CS} and thus δ_{obs} will increase with the cation ionic radius, each type should give a different contribution

(29) Mueller, K. T.; Wooten, E. W.; Pines, A. *J. Magn. Reson.* **1990**, *92*, 620.
(30) Greaves, G. N.; Gurman, S. J.; Catlow, C. R. A.; Chadwick, A. V.; Houde-Walter, S.; Henderson, C. M. B.; Dobson, B. R. *Philos. Mag. A* **1991**, *64*(5), 1059−1072.
(31) Soules, T. F. *J. Chem. Phys.* **1979**, *71*(11), 4570−4578.

to the spectrum of the mixed glasses. To be consistent with the known line shapes observed for $Si-O-Na_4$ (v-K_0 Na_{100}) and $Si-O-K_4$ (v-K_{100} Na_0) we can assume that those characteristic contributions will be of a Gaussian/Lorentzian type with a line width of ~900 Hz. This should take into account the cation−oxygen distance disorder, assuming it to be constant across all compositions. The non-observation of two resolved peaks for the nonbridging oxygen precludes a structural model with only two types of nonbridging oxygen sites (e.g., if significant clustering of alkali is occurring). If only two sites existed then the two 900 Hz wide peaks must have a separation of ~700 Hz (~13 ppm) in order to reproduce the ~1600 Hz observed line widths. This separation, however, would lead to a mixed glass spectrum that exhibits two maxima for the nonbridging oxygen site which is clearly not observed for the v-$K_{50}Na_{50}$ and v-$K_{25}Na_{75}$ compositions. One could also argue that the data are consistent with only one type of nonbridging oxygen existing in the mixed glasses and that as a result of the cation−oxygen distance disorder this nonbridging oxygen line width is increased when both compositions are mixed together. This argument, however, is not justified by EXAFS data[30] which show that the greatest cation−oxygen distance disorder in mixed alkali disilicate glasses is in the pure alkali composition of the alkali cation with the smallest radius, not the mixed alkali composition.

A structural model that is consistent with our results is the ideal solution model,[32] where the different alkali cations are distributed in random combinations around each nonbridging oxygen and it is assumed there is no energy change associated with a rearrangement of the K and Na cations. If this were the case we would expect the populations of the five different nonbridging oxygen environments to be dictated by the binomial distribution. According to the binomial distribution, the number of sites in which an environment $Si-O(Na_kK_{4-k})$ where $k = 0$, ..., 4 occurs in a glass of alkali composition $(Na_pK_{1-p})_2O{\cdot}2SiO_2$ ($0 \le p \le 1$) will be given by:

$$P(k) = \frac{4!}{k!(4-k)!}p^k(1-p)^{4-k} \qquad (3)$$

To test this model we simultaneously fit all five isotropic spectra in Figure 2 with the constraints that the relative intensity of each $Si-O(Na_kK_{4-k})$ component composing the nonbridging oxygen line shape follows the binomial distribution values dictated by the composition. Therefore, the simultaneous fit parameters describing all the nonbriding oxygen line shapes are the five positions and five widths of each $Si-O(Na_kK_{4-k})$ component, assuming that all components share the same Gaussian/Lorentzian line shape ratio. In addition, the bridging oxygen line shapes were all fit with the constraint that their line shapes have the same Gaussian/Lorentzian line shape ratio and that the bridging/nonbridging oxygen ratio be 60/40. The positions and widths of the bridging oxygens, however, were treated as independent fit parameters in each spectrum. In all, this is a 23 parameter simultaneous fit of all five spectra. The result of this fit is displayed on Figure 2 and detailed in Table 3.

It can be seen from Figure 2 that the resulting fit is in good agreement with the experimental spectrum and that a binomial distribution (i.e. ideal solution) of cations around the nonbridging oxygens is a reasonable approximation. It must be stressed that this is not the only possible interpretation; however, it is one which is very consistent with a simple structural picture of cations distributed in random combinations around the nonbridging oxygens, in agreement with Molecular Dynamics calculations[31] and deductions drawn from EXAFS results.[16] It must also be noted that one assumption in using eq 3 is that the probability of creating a $Si-ONa_kK_{4-k}$ species is independent of k (and therefore only dictated by the bulk composition). This may not be completely true since the various sites are not energetically equivalent: $Si-OK_4$ is more easily formed than $Si-ONa_4$ since the free energy of mixing for $K_2O{\cdot}2SiO_2$ is two times lower than the one for $Na_2O{\cdot}2SiO_2$.[33] This behavior could lead to small departures from the binomial distribution. One possible model that could be developed to account for these departures would be the central atom model.[32] In this model the configurational entropy is calculated assuming a random distribution of configurations $Si-ONa_k$ K_{4-k} and with each configuration assigned an energy the free energy is minimized to obtain the configurations' relative populations. Unfortunately, given the strong overlap of the resonances for the five oxygen environments it would be difficult to quantify energy differences between the different environments with any certainty. Fitting the data to look for deviations from a binomial distribution would lead to an overparametrized fit (i.e. a high correlation between parameter uncertainties). Therefore we have not pursued the development of this model for this particular set of data.

Table 3. Results of the fit Of the Isotropic Projection of the 2D ^{17}O DAS Spectra of (a) v-$K_{100}Na_0$, (b) v-$K_{75}Na_{25}$, (c) v-$K_{50}Na_{50}$, (d) v-$K_{25}Na_{75}$, and (e) v-K_0Na_{100} Assuming a Binomial Distribution of Nonbridging Oxygen Sites

bridging oxygen				nonbridging oxygen			
composition	δ (ppm)	$\Delta\nu$ (Hz)	G/L_{BO}	site type	δ (ppm)	$\Delta\nu$ (Hz)	G/L_{BO}
v-$K_{100}Na_0$	16.1	1271	0.69	K_4	68.7	896	0.94
v-$K_{75}Na_{25}$	16.0	1248	0.69	K_3Na_1	56.8	896	0.94
v-$K_{50}Na_{50}$	14.2	1396	0.69	K_2Na_2	45.4	896	0.94
v-$K_{25}Na_{75}$	13.9	1363	0.69	K_1Na_3	34.0	896	0.94
v-K_0Na_{100}	11.7	1276	0.69	Na_4	27.1	896	0.94

[a] δ is the position of the maximum, $\Delta\nu$ is the full width at half maximum, $x = G/L$ refers to the $x \times$ Gaussian $+ (1 - x) \times$ *Lorentzian* shape. χ^2 reduced for this fit is $\chi^2_\nu = 6.46$.

It is interesting to compare these results with previous ^{17}O DAS NMR experiments performed on v-$K_2Si_4O_9$ and v-$KMg_{0.5}Si_4O_9$[8] which have shown an ordering of potassium and magnesium around the nonbridging oxygen. The large differences in cation charge/radius ratio (Na^+, ~1.00 Å; K^+, ~1.38 Å; Mg^{2+}, ~0.49 Å[27]) probably have an effect on their ordering in glassy silicates. This contrast in cation ordering in the mixed K,Mg and K,Na glasses is sensible in light of the existence of the ordered crystalline compound $K_2O{\cdot}MgO{\cdot}5SiO_2$,[34] while no ordered crystalline compounds in the K,Na system are known to exist. It should also be pointed out that the K,Mg ordering in the glass is not only mimicked by the crystalline phases but is sensible in that the two cations may have very different coordination "demands" (8−10 for K, 4−6 for Mg).

Conclusions

^{17}O Dynamic-Angle Spinning NMR experiments on the five disilicate glass compositions $K_2O{\cdot}2SiO_2$, $(Na_{0.25}K_{0.75})_2O{\cdot}2SiO_2$, $(Na_{0.50}K_{0.50})_2O{\cdot}2SiO_2$, $(Na_{0.75}K_{0.25})_2O{\cdot}2SiO_2$, and $Na_2O{\cdot}2SiO_2$,

(32) Lupis, C. H. P. *Chemical Thermodynamics of Materials*; P. T. R. Prentice Hall: Englewood Cliffs, NJ, 1983.

(33) Charles, R. J. *J. Am. Ceram. Soc.* **1967**, *50*, 631.

(34) Levin, E. M.; Robbins, C. R.; McMurdie, H. F. *Phase Diagrams for Ceramists*; The American Ceramic Society: Westerville, OH, 1964.

provide a unique view of the alkali cation ordering around nonbridging oxygens in silicate glasses. Results presented here show high resolution oxygen spectra that are consistent with a random mixing of two alkali types on four sites around each nonbridging oxygen. These results preclude significant clustering of similar cation types and are generally supportive of models of the mixed alkali effect that involve blocking of cation migration pathways by "foreign" cations.[16,18]

Acknowledgment. We thank Jay Baltisberger and Ulrike Werner for assistance in the preliminary stages of this work. This work was supported in part by the National Science Foundation, through Grant No. CHE-9501872 to P.J.G.

JA953918C